

Behavior of the Cryogenic Propellant Tanks during the First Flight of the Ariane 5 ESC-A Upper Stage

Philipp Behruzi* and Mark Michaelis†
EADS Space Transportation, 28209 Bremen, Germany

and

Gaël Khimeche‡
EADS Astrium, 31402 Toulouse Cedex 4, France

On February 12th 2005 the first flight of the new Ariane 5 cryogenic upper stage was successfully carried out. In the frame of a post-mission analysis the flight data has been evaluated in detail in order to investigate the propellant and thermodynamic behavior during the flight. Goal of the analysis is thus to understand the behavior of the propellant in the tanks and to study the accuracy of the applied numerical tools. During the flight assessment the whole mission, starting on the launch pad until passivation of the stage, has been examined. The document highlights certain mission phases such as the ballistic phase (separation of the payload) and the passivation phase. The passivation phase consists of a tank pressure reduction in order to avoid an uncontrolled later explosion. Various sensors inside the propellant tanks allow a correlation of the propellant location in the tanks with the performed numerical CFD predictions. The numerical analyses were carried out with the FLOW-3D® software¹ to simulate propellant sloshing and an in-house software for the thermodynamic behavior. The analyses demonstrate the capability of the numerical analyses to better understand the propellant behavior in the tanks, which is an advantage for future upper stage developments.

Nomenclature

P_{ullage}	=	Ullage pressure
P, p	=	roll angular velocity around x axis
Q, q	=	nick angular velocity around y axis
R, r	=	yaw angular velocity around z axis
t	=	time
T	=	Temperature

I. Introduction

THE first flight of the new Ariane 5 cryogenic upper stage ESC-A occurred February 12th 2005. A picture of the Ariane 5 including the upper stage ESC-A is shown in Fig. 1. The post-mission analysis addresses the main flight sequences which are:

- the boost phase of the solid boosters together with the first lower liquid propelled stage until separation of the solid boosters
- the flight phase of the first stage
- the separation of the upper stage after burnout of the first stage
- the upper stage flight phase
- the cut-off of the upper stage and the preceding ballistic phase including the release of the payload
- the passivation of the upper stage.

* Engineer, Fluid Dynamics, Mechanical Engineering, Philipp.Behrui@space.eads.net, Member AIAA.

† Engineer, Fluid Dynamics, Mechanical Engineering, Mark.Michaelis@space.eads.net.

‡ Engineer, Fluid Dynamics, Mechanical Engineering, Gael.Khimeche@astrium.eads.net



Figure 1. First launch of the Ariane 5 (flight V521) and the upper stage ESC-A

Two main mission phases are discussed more closely, i.e. the ballistic phase including the release of the payload and the adjacent passivation phase. Both flight phases are of great interest due to the complex propellant motion in the tanks.

The Reaction Control System (RCS) uses a cold gas system to perform the attitude control during the propulsive phase and the ballistic phase (payload separation phase) as well. Four pods, each of them equipped with three electro-valves and three thrusters are connected to the hydrogen tank (see Fig. 2). They allow control of the launcher. The longitudinal acceleration, required to move away from the payloads after separation, is provided by thrusters connected to the oxygen tank.

Such a cold gas system does not provide a constant thrust over the mission since it depends on the pressure and temperature conditions inside the propellant tanks. It is mandatory to predict correctly the thrust level over the mission since the controller has to have the correct thrust characteristics. Therefore it is of importance to master the thermodynamic behavior of the propellant tanks (pressure and temperature conditions) and the propellant position regarding a possible liquid ingestion into the thrusters.

In a first step the thermodynamic behavior of the propellant tanks is thus analyzed. The second step focuses on the propellant sloshing behavior.

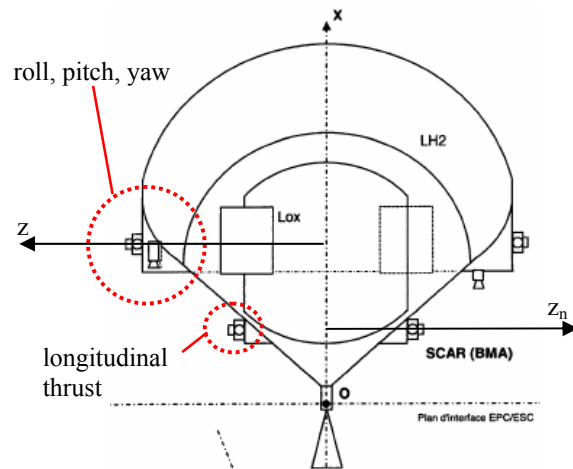


Figure 2. Attitude control system of upper-stage

II. Thermodynamic model for the ballistic phase including release of the payload

The applied thermodynamic model is structured to analyze a complete propulsion upper stage with its components. The used in house analysis tool evaluates the stage behavior and the resulting stage performance during all mission phases (ground, propulsive and ballistic phases). The model is able to take into account all relevant parts of the pressurization system (relief valves, pressure regulators, helium vessels, ...), the feeding system (turbo pumps, turbine, engine, gas generator, ...) and the propellant tanks (oxidizer and fuel as propellant). A specific part of the model deals with the propellant tanks which are divided into a gas phase and a liquid phase.

A. Modelization details

The state in the bulk of the tanks (liquid and gaseous phase) is characterized by a uniform state using only the time dependent formulation of the conservation laws.

Within the liquid the following physical phenomena are considered:

- the heat exchange between the wall and the liquid phase is considered as
 - natural convection in case of a sub-cooled propellant
 - liquid boiling under several conditions (nucleate, transient and film boiling)
- the overall boiling induced by a pressure drop in a saturated liquid
- the condensation of propellant vapor in a sub-cooled liquid

Within the ullage:

- the heat exchange between the wall and the gaseous phase considered as
 - natural convection for the stand-by phases (no pressurization)
 - forced convection for the pressurization phases (ground and flight)
- the condensation of propellant vapors on the inner side of the wall

At the propellant free surface:

- the heat transfer as
 - natural convection for the stand-by phases (no pressurization)
 - forced convection for the pressurization phases (ground and flight)
- the mass transfer by evaluating the vapor pressure difference

Within the tank structure

- pure conduction in non-porous materials, otherwise convection and radiation
- external heat fluxes via convection on ground and solar, earth and structure radiation in orbit

The model does not consider propellant sloshing but is able to work under two configurations:

- longitudinal acceleration with the propellant settled at the tank bottom
- spin environment around the launcher axis with the propellant located on the external tank walls

A flow schematic of the used thermodynamic model is shown in Fig. 3.

Depending on the state of the tanks, i.e. pressurization or outgassing phase, either the segregated solution path (left column) or the coupled solution path (right column) is used applying an implicit time integration with adaptive time step adjustments. The pressure is monitored when sufficient accuracy is reached.

The model was used to issue the predictions for the first flight. Using the flight measurements, the model was then improved in order to consider some effects which have not been taken into account before such as:

- the impact of propellant sloshing on the evaporation flow rate
- the impact of the lines going to the thrusters via their thermal inertia
- the impact of the low acceleration levels on the heat exchange inside the propellant tanks.

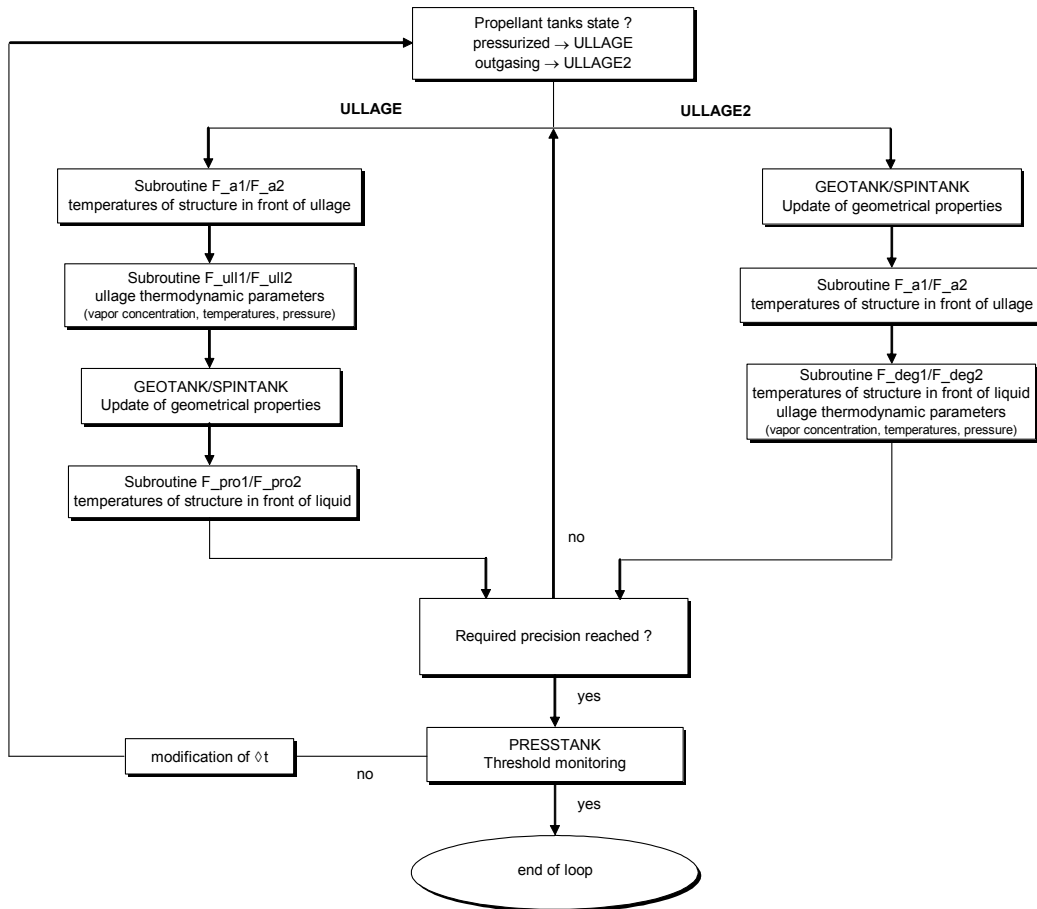


Fig. 3. Flow schematic of the thermodynamic model

The results of this correlation are presented in Fig. 4.

Six sub phases can be distinguished:

1. Upper payload separation (1500-1600 s)
2. Payload adapter structure separation (1600-1700 s)
3. Lower payload separation (1700-2000 s)
4. Zero-g environment (2000-2300 s)
5. Preparation of stage passivation (2300-3200 s)
6. Propellant tank passivation (>3200 s)

The first three phases consist of orientation maneuvers to set the chosen direction for each payload jettisoning. The zero-g environment (phase 4) provides useful information concerning the heat fluxes entering the propellant tanks and the associated thermal environment of the upper composite. During the fifth phase (preparation for passivation) the upper composite is spinned up. Thus the liquid will be driven away from the diffuser. The last phase is the passivation phase. The propellant tanks are then depressurized to avoid any later explosion.

The predicted pressure evolution was well estimated by the numerical model compared to the flight data.

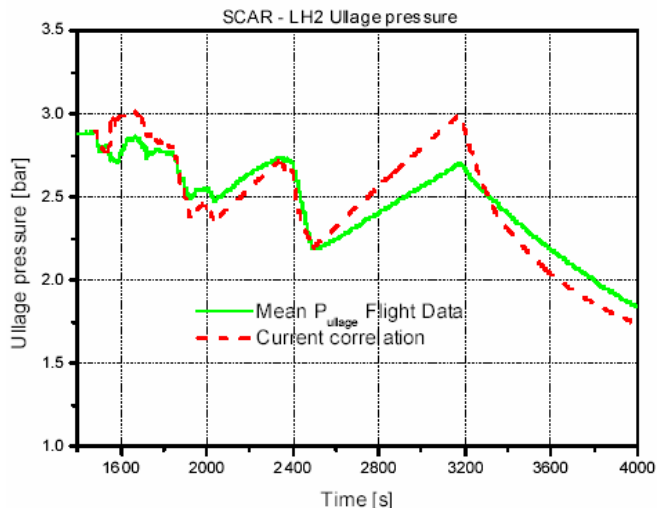


Figure 4. Pressure evolution in hydrogen tank during first flight

III. Propellant behavior during the ballistic phase

After engine shutdown the propellant is assumed to be initially located at the bottom of the tanks with an initially flat free surface (see Fig. 5) as a consequence of the preceding thrust phase.

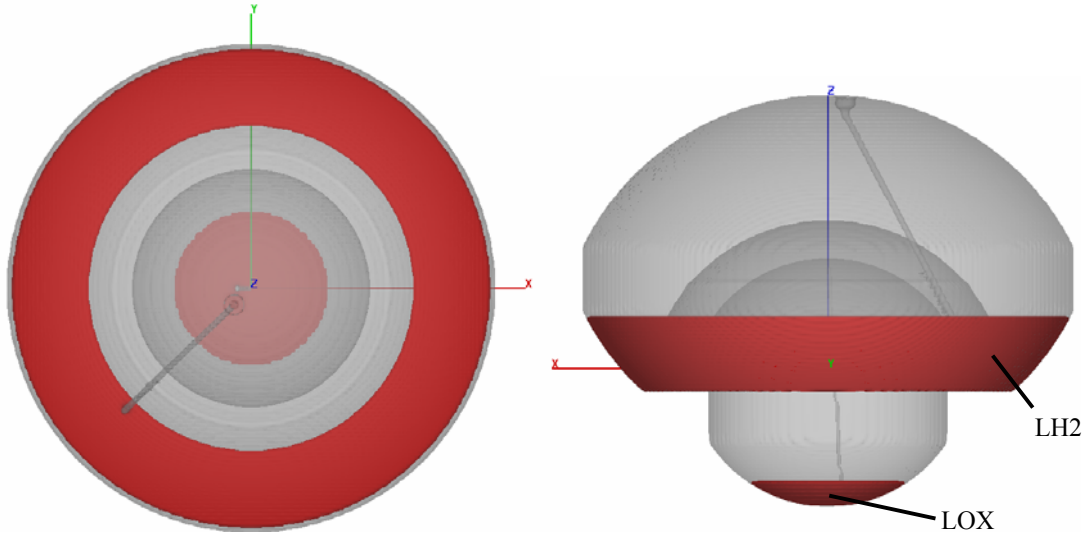


Figure 5. Initial location of propellant inside the ESC-A tanks (left hand side: top view on the tanks from above, right hand side: side view on the tanks).

The following ballistic phase consists of a number of redirection maneuvers and a spin-up phase of the stage to $10^\circ/\text{s}$ for P/L release as shown in Fig. 6, $t = 1900$ seconds after lift-off. At $t = 2400$ seconds a spin-up phase occurs followed by a passivation of the system at high spin rates. Several temperature sensors have been implemented in and around the tank to provide information concerning the propellant stratification. During the ballistic phase these transducers can be used as liquid markers in order to assess the liquid location in the tanks. The different sensors were introduced into the FLOW-3D[®] model in order to enable a comparison with the flight data. The ESC-A tank model, used in the frame of the FLOW-3D[®] calculation, is shown in Fig. 5.

An example of a comparison between the measured temperature profile and the corresponding numerically estimated wetting condition at the same location is shown in Fig. 7. The sensor is located at the outer wall of the upper bulkhead structure. The history data with respect to the sensor temperature and the fluid fraction estimated by the numerical analysis is given. A fluid fraction of one corresponds to a totally wetted cell and a fluid fraction of zero to the absence of liquid. The first liquid wave reaches the sensor around $t = 1600$ seconds (point number 1 in Fig. 7) which leads to a temperature decay. The sensor slowly cools down since the cold liquid reaches the sensor. Around $t = 2080$ seconds (point number 2 in Fig. 7, see dashed temperature curve) the sensor temperature drops to the liquid temperature because the sensor location is then about constantly covered with liquid (fluid fraction mostly near one). Thus the sensor stays at liquid temperatures.

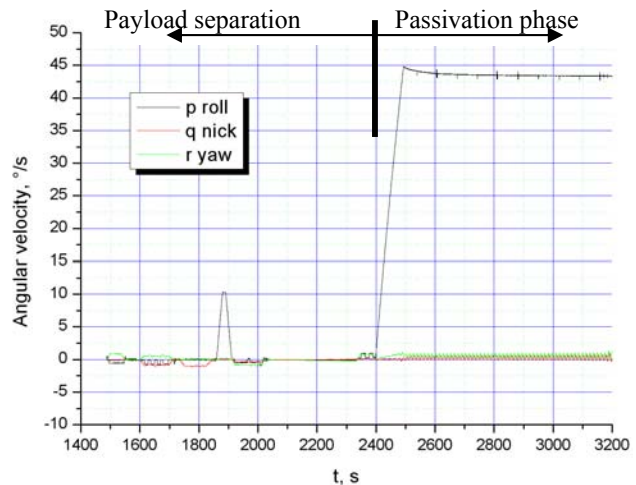


Figure 6. Angular velocity profile during ballistic phase with payload release

Figure 8 shows the location of the propellant during certain instances of the payload separation phase. The analyses show that liquid may reach the diffuser located at the tank top. The diffuser system is used to provide the thrust for the reaction control system. Thus it had to be ensured that liquid ingestion into the diffuser system does not affect the efficiency of the attitude control.

For this specific purpose a two-phase flow model was built in order to assess the flow properties inside the lines up to the attitude thrusters. It turns out that the notion of the critical mass flow still exists for a two-phase flow. In single phase systems, the flow velocity becomes equal to the sound velocity (Mach number equal to 1). This relationship between sound velocity and critical mass flux in two-phase systems is less direct, the sound speed being a function of the two-phase flow pattern and of the sound velocity.

The model consists of a fine discretization of the pipe in which the two-phase flow takes place. The major physical parameters are:

- the propellant tank pressure
- the void fraction at the pipe inlet
- the internal pipe temperature
- the pressure drop inside the pipe
- the external thermal environment.

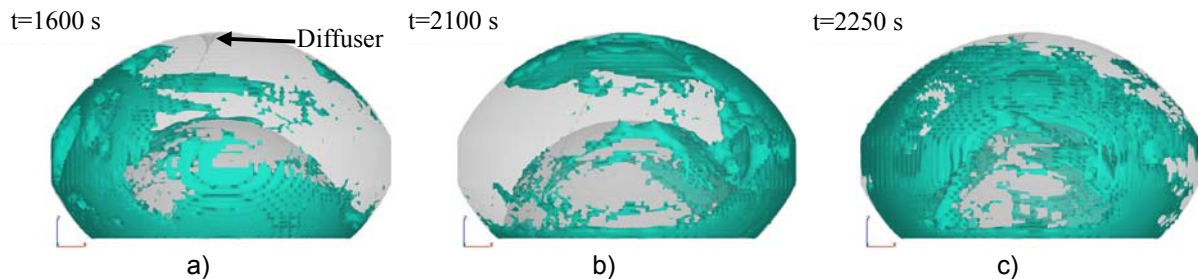


Figure 8. Location of propellant at different times after beginning of the payload separation phase (t = 1600s, t = 2100 s and t = 2250 s)

The model is then able to forecast the amount of fluid which vaporizes inside the pipe and the associated pressure loss. This pressure drop drives the expelled mass flow out of the thrusters.

Figure 9 depicts the impact of liquid ingestion on the delivered thrust. The nominal thrust with pure gaseous hydrogen is about 58 N. The thrust decreases suddenly as soon as liquid ingestion occurs. This effect is due to the filling of the lines with propellant. Then the thrust rises above the one that would be delivered considering pure gas and decreases slowly.

The thrust variations caused by the propellant ingestion do not jeopardize the

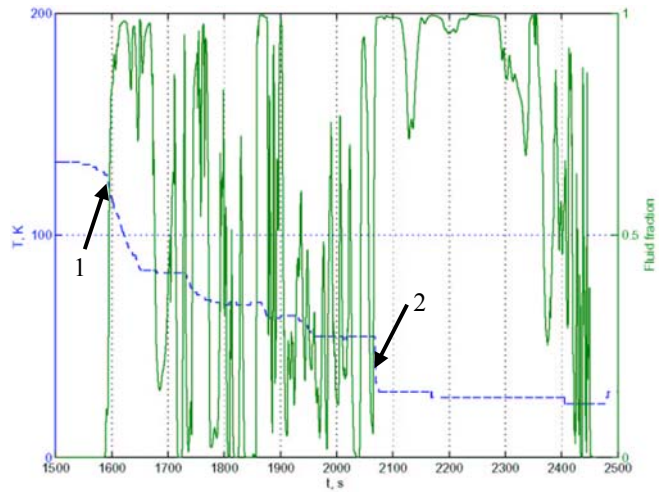


Figure 7. Temperature history profile of a sensor in the LH2 tank and fluid fraction history profile from the numerical calculation (fluid fraction = 1 corresponds to a cell totally covered with liquid, fluid fraction = 0 corresponds to only gas in cell -- liquid temperature is lower than 24 K)

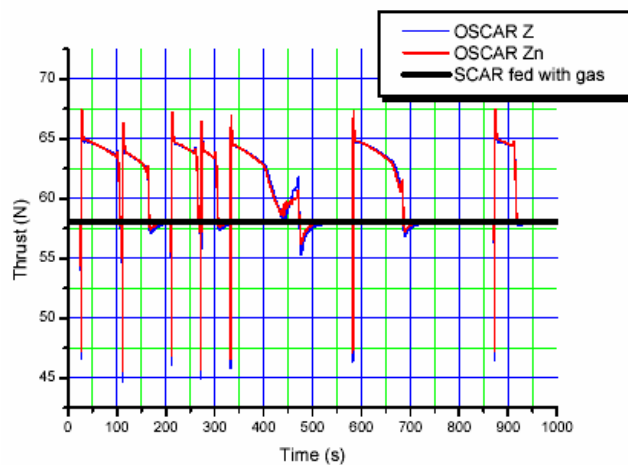


Figure 9. Thrust profile in case of liquid ingestion

attitude control of the upper stage since they remain less than two times the thrust provided by pure gas. This value is considered to be the limit which should not be exceeded to ensure launcher stability.

IV. Passivation of the ESC-A Upper Stage

The passivation of the upper stage occurs some time after separation of the payload. Initially the liquid is in a state of motion as a consequence of the preceding ballistic payload separation phase. The location of the propellant in the tank prior to passivation is shown in Fig. 10.

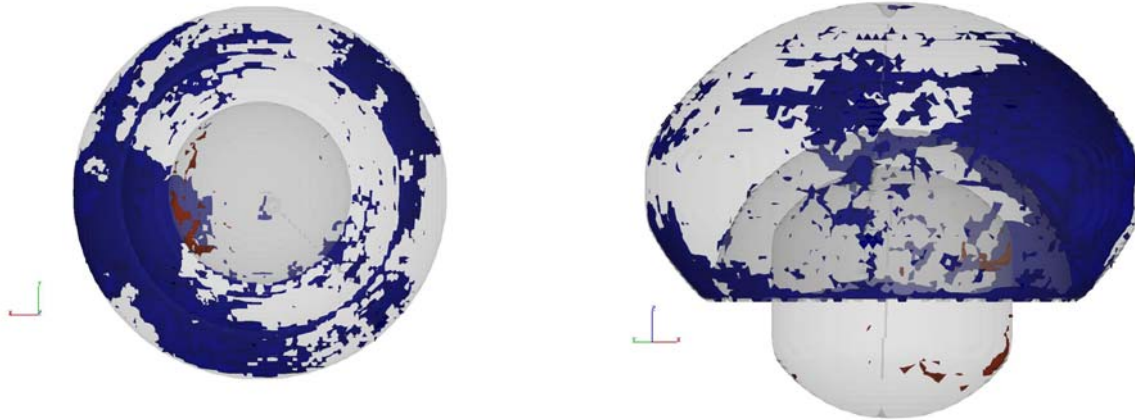


Figure 10. Initial location of propellant inside the tanks (left hand side: top view on the tanks from above, right hand side: side view on the tanks).

The passivation phase is initiated by a spin-up to about $45^\circ/\text{s}$ ($t \approx 2500$ seconds after lift off, shown in Fig. 11). After spin-up of the spacecraft the RCS is not used any more. Thus goal of the passivation phase analyses were the prediction of the spacecraft motion influenced by the sloshing motion in the tank. This was analyzed by carrying out a coupled propellant / rigid body open loop simulation (without control algorithm) (see also Ref. 2). Since the motion of the spacecraft is not any more controlled it was observed that the stage slowly tends towards flat spin motion as a consequence of the magnitudes of the main spacecraft moments of inertia. The same phenomenon was predicted by the numerical analyses.

Two different coupled open loop numerical models were applied. The first model is the rigid body model as provided by FLOW-3D[®] (see Ref. 1). The second model is an in-house simulation tool called Final Phase Simulation Tool (FIPS)^{3,4} which has been coupled with FLOW-3D[®]. The tool is able to carry out open loop as well as closed loop simulations. One advantage of the FIPS code is the possibility to have access to the FLOW-3D[®] output data before passing it to FIPS. Thus it is possible to check and if necessary to filter the output data ensuring that no numerical disturbances influence the rigid body motion. A simplified schematic representation of the interaction between FIPS and FLOW-3D[®] is shown in Fig. 12. The rigid body model exchanges acceleration as well as force and torque data with the fluid dynamic model. Furthermore simplified models, such as spring-mass models can be coupled to FIPS in the same manner as done with the FLOW-3D[®] model in the present case. FIPS is thus very flexible and also able to take into account the control algorithm during flight (not required for the passivation analyses).

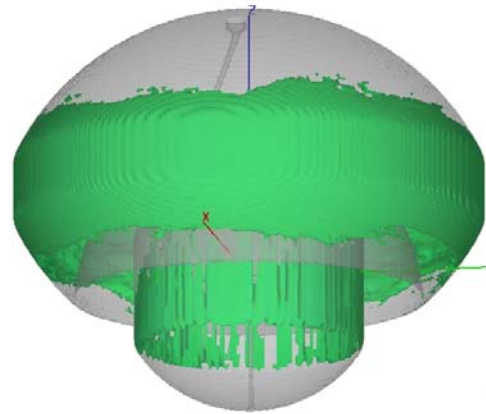


Figure 11. Propellant location in the two ESC-A tanks 360 seconds after spin-up

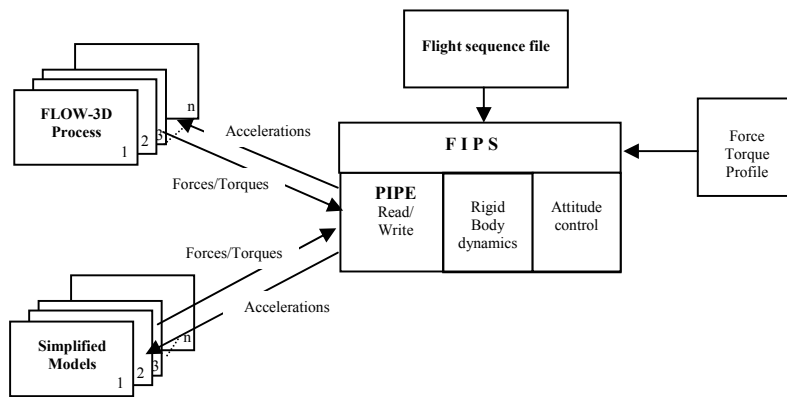


Figure 12. Simplified representation of the interaction between the rigid body model and the FLOW-3D® model through FIPS

Using the ESC-A flight data an estimation with respect to the accuracy of the two models was carried out. Figure 13 shows the propellant location in the tanks for dedicated time steps applying the internal FLOW-3D® model. In a first step the liquid was assumed to be initially located at the tank bottom in order to have a clearly defined simple initial condition before spin-up.

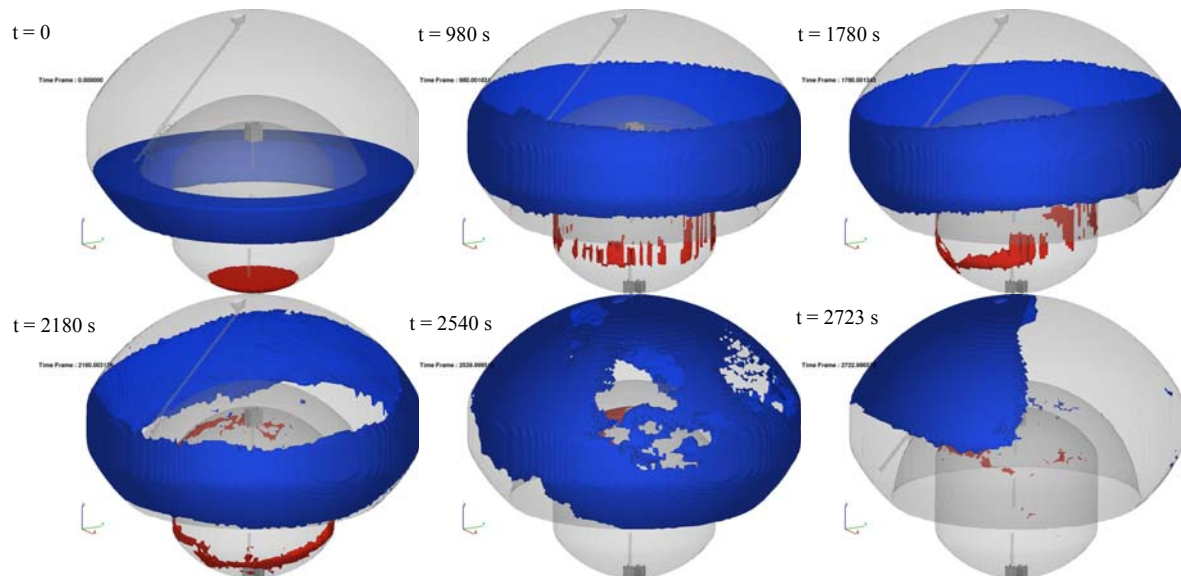


Figure 13. Propellant location in the tanks for dedicated time steps using the internal FLOW-3D® model (t = 0 corresponds to the beginning of the passivation phase prior to spin up)

Due to the inertia of the rotating fluid the liquids inside the tanks keep a stable ring shape after spin-up while the stage slewing angle grows with time. Finally the slewing angle of the stage is large enough for the LH2 in the upper tank to get in contact with the intermediate bottom structure leading to large splashing (t = 2540 s). The internally coupled FLOW-3D® model then estimated that the propellants in the tanks gather at the tank top (t = 2723 s). This behavior was neither observed during flight nor expected since the center of mass is located above the tanks which should drive the liquid towards the tank bottom in case of near flat spin motions. The correct final propellant location was however reproduced by the second coupling method using FIPS. Here the propellant was finally located stable at the tank bottom. We expect that the filtering of the numerically generated disturbances is mainly responsible for the improved result. All numerically generated pressure peaks directly lead to an additional (unphysical) acceleration impulse if not filtered.

The angular velocities (numerical FLOW-3D® results and flight data) in longitudinal and transversal direction corresponding to Fig. 13 are shown in Fig. 14.

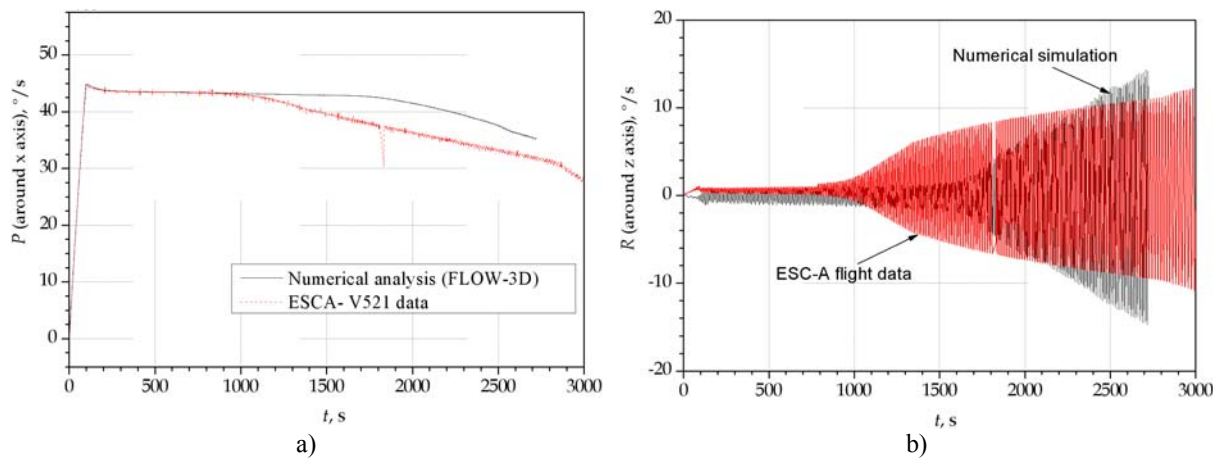


Figure 14. Comparison of the FLOW-3D® results with the ESC-A flight data -- a) of the angular velocities around the longitudinal axis, b) of the angular velocities around the transversal axis ($t = 0$ corresponds to the beginning of the spin up)

It can be seen that the spin rate of the stage during passivation is very well reproduced by the numerical results during the first 1000 seconds. After this time a significant slewing motion starts with increasing amplitudes (see ESC-A flight data in Fig. 14, right hand side picture). The increased slewing rate is delayed for another 600 seconds in the numerical analysis. However the profiles show the same characteristics which enable a good understanding of the behavior in the tanks. In the present numerical analysis the initial location of the liquid at the tank bottom leads to a more homogeneous propellant distribution during spin up. Thus the required time until the slewing motion starts is delayed. The real propellant location is expected to be similar to the situation stated in Fig. 10.

The deviation of the propellant location compared to the flight case after about $t = 2700$ seconds then also leads to a deviation of the slewing rate as well as the spin rate.

The second numerical model using FIPS enables the observation of the propellant behavior when the LH2 reaches the intermediate LH2 tank bottom (see Fig. 15).

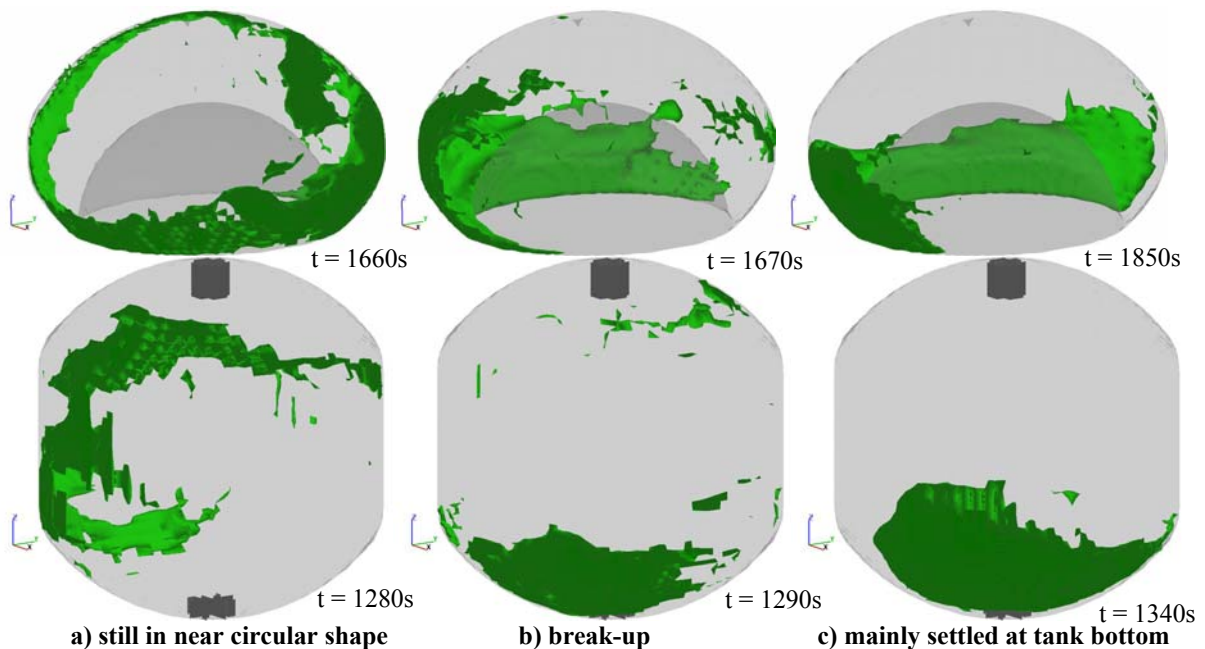


Figure 15. Propellant location inside the LH2 tank (top) and the LOX tank (bottom) when the transition from a circular ring shape fluid motion to a mainly settled motion occurs (FIPS simulation).

Similar to the behavior in the LH2 tank the LOX also settles at the tank bottom, only slightly earlier in time. The time frames differ compared to the above internal FLOW-3D[®] calculation since the breakup occurs earlier in this calculation. The main characteristics of the history profiles are however the same. It can be seen that the liquids tends toward the tank bottom both for LH2 and LOX, as expected, and stays there until all liquid is evaporated during passivation of the tanks.

V. Conclusion

The present analysis provides an overview of the propellant behavior occurring in the Ariane 5 ESC-A tank during its maiden flight on February 12th 2005. The comparisons which were carried out for the analysis of the mission phases enable a good understanding of the propellant behavior. Two mission phases are analyzed in detail in the present paper:

1. The ballistic phase during payload separation. In this phase the RCS thrusters are activated numerous times leading to large sloshing motions in the tanks.
2. The final passivation of the spacecraft. During passivation all tanks will be depressurized. The spacecraft is left uncontrolled during this phase.

Numerical analyses were carried out for both phases, mainly using the commercial FLOW-3D[®] software¹. During passivation the RCS of the stage is not any more active. Thus a coupled fluid dynamics / rigid body analysis was used. The applied numerical tools turned out to be suitable for the estimation of the propellant behavior. The location of the propellant inside the tanks was predicted accurately enough for the layout of spacecrafts. Thus they can be used as design tools for future cryogenic upper stages, e.g. for a next generation of restartable upper stages with long ballistic phases.

References

- ¹FLOW-3D[®], Flow Science Inc., <http://www.flow3d.com>
- ²Behruzi, P., Bellec, G., Dufour, A., and Marichal, B., "Sloshing and GNC Coupling Methodology in EADS Space Transportation", *EUCASS Europ. Conf. for Aerosp. Sci.*, Moscow, July 2005
- ³Klotz, H., Burkert, R, and De Rose, F., "Coupling Dynamic Simulations of Spacecraft Containing Liquids", *FLOW-3D User's Conference*, Santa Fe, Sept. 1999
- ⁴Klotz, H., and Burkert, R, "Coupled Flow-3D Simulation for Analysis & Modelling of Dynamics of Upper Stages Containing Liquids", *5th Int. Conf. on Launcher Techn.*, Madrid, Nov. 2003